Predoctoral year of research

Development of a shake table addon to reproduce Tohoku earthquake ground motions on constructions

under the direction of Pr. Kawase (DPRI), As. Pr. Matsushima (DPRI) and Pr. Ragueneau (ENS)
Disaster Prevention and Research Institute, Kawase & Matsushima laboratory, Kyoto University

Final report

written by

Vincent CROZET

Kyoto university, Uji campus
Gokasho, Uji-shi, Kyoto-fu, 611-0011

Contents

List of Figures

1 Introduction

Within the study of ground motions and their relation to observed structural damages during the 2011 Off the Pacific Coast of Tohoku earthquake, a mean to reproduce strong ground motions recorded during this event has been studied. The uncommon rupture area estimated to 500 km long by 200 km width and the released energy Mw 9.0 created strong ground motions widely in Japan, with a PGA of 2700 gal (cm/s^{2}0 for NS component and 2900 gal for vectorized sum acceleration occurring in Miyagi prefecture at a K-Net site called MYG004 (Tsukidate area). However, despite the intensity of the recorded ground motions the damage in this area were quite low and mainly consisted in non-structural parts of the infrastructure damages such as roof tiles fall and broken windows. The unpredictability of such observation as well as the difficulty to understand the extreme earthquake events lead to discussion and questioning about : the trustworthy of the recorded ground motions at MYG004 and the specificity of the geological structure in Tsukidate area that will be discussed in part 2.1. Moreover the inconsistency of Japanese JMA intensity scale with building damage observation around K-Net site MYG004 brought strong doubt to people living in Japan about the accuracy of such an intensity scale. This questioning about JMA intensity scale was discussed in the mid term report. Therefore it was aimed to reproduce by the use of a shake table the ground motions recorded at MYG004 on a wooden frame to provide information about the Japanese traditional wood frame behavior under such severe condition.

This goal suffer from an important drawback as common shake table cannot perform such a high acceleration. Indeed Kyoto university shake table can reproduce ground motions with a maximum acceleration up to 1 g, 981 gal. Consequently possibilities to create a flexible structure able to amplify the shake table acceleration in a specific frequency range was investigate. This structure use resonance of one degree of freedom oscillator in order to provide the amplification. The development of this structure and the wood frame experimental results will be exposed in part 3 and 5.

This report will present the advancement on this project performed at Kyoto University since October 2014 in the Disaster Prevention and Research Institute. It will mainly show achievement performed form April 2015 to August 2015, since study completed from October 2014 to April 2015 has been documented in the mid-term report.

2 Ground motions analysis of Tohoku earthquake

This section intend at briefly sum up the ground motions specificity that have been discussed in the mid term report and also present discussion and further work performed in the context of explaining the peculiarity of MYG004 ground motions.

2.1 Specificity of Miyagi prefecture ground motions recorded during Tohoku earthquake

Tohoku earthquake is qualified as megathrust event due to the important fracture area and the big stress drop that occurred. The slip process modeling using waveform inversion techniques was detailed in the mid term report and is well presented in the litterature [9]-[13]. This fracture process created strong ground motions in Japan, since 18 KiK-net and K-NET recorded PGA of more than 1g as a PGA verctorized sum.

The strongest recorded ground motions are gathered in Miyagi prefecture were the maximum horizontal acceleration ever recorded in Japan occurred at a K-NET site called MYG004 Tsukidate with a value of 2700 gal considering the North-South component. Nevertheless, no structural damage were observed around this site and most important damage in Miyagi prefecture gathered around MYG006 site located about 17 km away from MYG004 site. The contrast of damage occurrence linked with recorded ground motions in Miyagi is important as MYG006 K-NET site recorded maximum acceleration of 583 gal. This contrast is also appearing in the JMA intensity as MYG004 was the only site to record JMA intensity 7. This is a scale used in Japan principally by population to evaluate the threat of ground motions to people, detailed explanation about JMA intensity were given in the midterm report and are found in the literature [19]. The ground motions recorded at MYG004 and its acceleration spectra are shown figure 1. These ground motions are characterized by two wave packet, where second wave packet show strong acceleration in both UD and NS component. The strongly oriented amplification is inducing a specific soil condition due geology or topography. Moreover the ground motions at MYG004, Tsukidate, show unusual high frequency content with a predominant frequency of 5 Hz. This contrast of frequency can be seen figure 2 comparing pseudo-velocity response of MYG004 with other sites located close to the Pacific coast such as MYG006 as well as other earthquake data. The location of the K-Net sites, which are mentioned figure 2, is shown figure 3.

It appears that the shape of the peak figure 2 is consistent with the structural damages as damaged occurred on structures at MYG006 site and 4b9 site (less than 2 km away from MYG006) and have close frequency content in the frequency band from 0.5 s to 2 s as 1995 Kobe earthquake in Takatori and 2004 Niigataken-Chuetsu earthquake in Kawaguchi pseudo-velocity responce spectra. Both these data from past earthquake refers to highly damaged areas after earthquake events [14]-[18]. The detailed damage report about sites MYG004 and MYG006 are found in the literature [1]-[4].

2.2 Study of the soil configuration around MYG004

As it has been shown in the previous section the ground motions recorded at MYG004 are inducing a strong site amplification and influence of the topology or geology. These characteristics were studied in the DPRI, Kawase sensei and Matsushima sensei laboratory by Nagashima [6],[7]. The high frequency content of the ground motions supposed a strong influence of the shallow layers of the soil. In fact site amplification at MYG004 could be strongly influenced by the presence of a small hill and an artificial cliff about 5 m high, due to the construction of a parking lot as it can be seen figure 4 and 5 . The hills and cliffs as well as close presence of free surface for refraction are known to be possible source of complex soil nonlinearity [8].

Theses nonlinearities were studied using aftershock at MYG004 site and close to this site [6],[7] as well as using microtremor array measurements [5]. The study of aftersock at MYG004 showed a strong

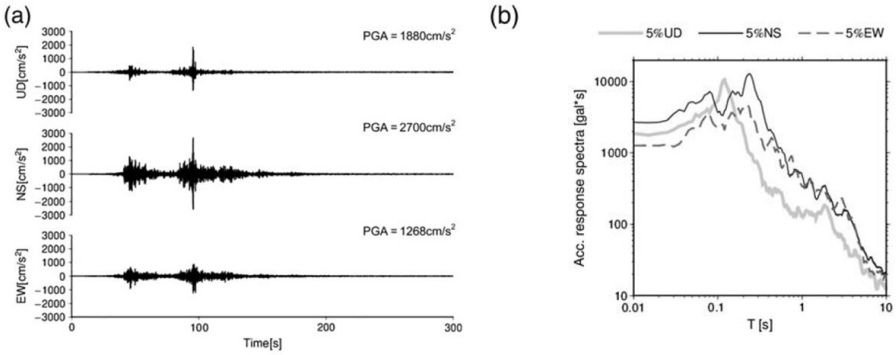

Figure 1: Ground motions characteristics recorded at MYG004 during 2011 Tohoku earthquake [6]. a) Acceleration time history. b) Acceleration response spectra with 5% damping.

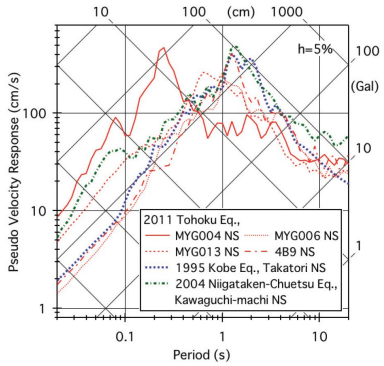

Figure 2: Pseudo-velocity response spectra for Tohoku earthquake Miyagi prefecture sites and other meaningful earthquake events [3].

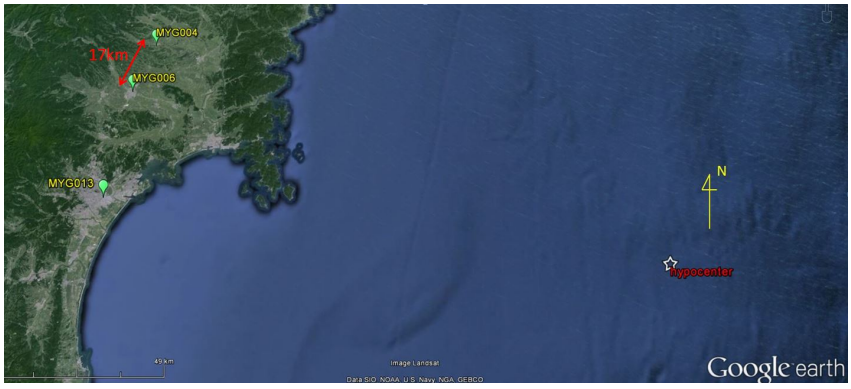

Figure 3: Location of considered site along the Pacific coast.

nonlinearity of the soil depending on the intensity of the ground motions. This purpose is shown figure 7 comparing the average H/V spectral ratio of aftershock recorded from March to September 2011 except for the maximum PGA aftershock (that occurred 7^{th} April 2011) and the mainshock of 11^{th} March 2011 with H/V of strong ground motions data. H/V spectral ratio correspond to the ratio between the horizontally recorded acceleration spectra with the vertically recorded acceleration spectra. It is seen that the predominant frequency of the H/V spectral ratio notably decrease for NS component from 9 Hz for weak motion to 5 Hz in the case of high PGA, instead the impact of the intensity of the ground shaking is inferior for the EW component. In addition to the frequency decrease the amplitude of the H/V spectral ratio increase which is not common for soil nonlinearity. This behavior was found to happen in case of specific shallow soil structure by Kawase [20] and is consistent with the soil structure calculated with H/V spectral ratio by Nakashima.

Moreover the study of aftershock in temporary station in a radius of less than 3 km around MYG004, as shown figure 5 (station location TKDZ01 to TKDZ04), account for a local site amplification at MYG004 creating this specific high frequency amplification. Figure 6 shows the disparity of the predominant frequencies in the H/V spectral ratio for the different stations and considering weak aftershock. MYG004 site show high predominant frequency for the NS component with a value of 9 Hz, instead site TKDZ04 show medium predominant frequency around 2.5 Hz. As for previous study, the contrast of the high frequency site amplification suggest an important influence of the shallow soil structure which can be related to the topography and peculiarly to the small cliff at MYG004. Nevertheless all sites show peaks at 0.3 Hz and 1 Hz which suppose an homogeneous deep soil structure. In addition, the lower predominant frequency at TKDZ04 compared to other sites could be related to nonstructural damage observation. Indeed some non structural damaged such as toppled lantern, broken windows and roof tiles fall occured around the TKDZ04 site in Tsukidate area [1].

To conclude MYG004 site shows important soil nonlinearity due to topography that can account for the strong ground motions that have been recorded. Moreover the low observed structural damage observed around MYG004 in Tsukidate area could be explain by a strong spatial heterogeneity of the site amplification. This heterogeneity might have generate strong ground motions in an area with a radius within some hundred meters.

Figure 4: Parking lot close to MYG004

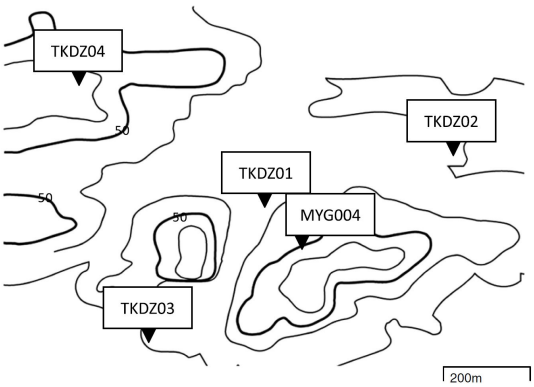

Figure 5: Topology around MYG004 [6]

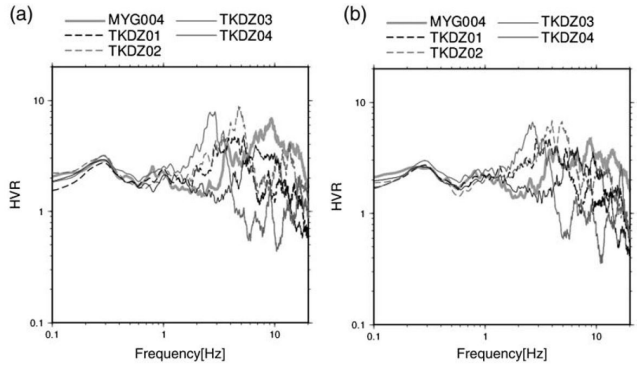

Figure 7: H/V spectral ratio of weak aftershocks at MYG004 close to this station. a) NS/UD. b) EW/UD.[6]

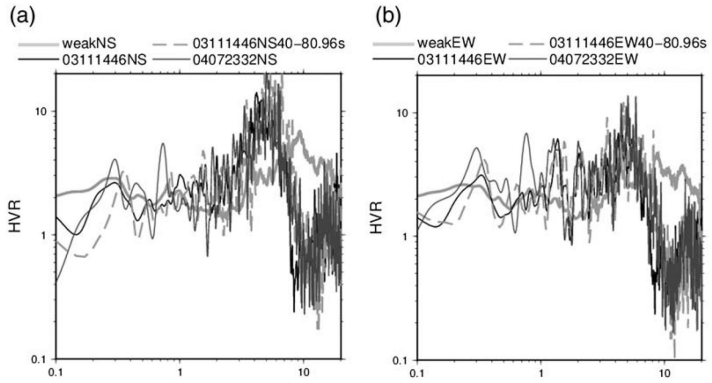

Figure 6: Comparison of H/V spectral ratio for weak aftershock (weakNS), main shock (03111446NS), and maximum PGA aftershock(04072332NS)[6]

2.3 Reliability of record at MYG004

Futhermore some studies [3]-[5] queried about the reliability of the recording at MYG004 suspecting some uplifting of the seismometer basement that could be the source of the sharp peak seen in MYG004 data. As a first observation it can be seen on figure 8 that MYG004 is one of the only site showing such a sharp peak for tha NS component (station MYG013 also show a sharp peak of 1500 gal). The closest from MYG004 considered station in Motosaka study along the Pacific coast are MYG006 and IWT012 showing respectively 445 gal and 590 gal for NS component PGA.

Moreover based on a questionnaire which correspond to former evaluation of the JMA intensity, Motosaka showed that former JMA intensity scale would have evaluated the ground motions intenstity around Tsukidate with a value of 5.6. The difference between former and actual JMA intensity scale was explain in the midterm report, it can be sum up as the former JMA intensity scale was based on observed structural damage and felt ground motions due to an earthquake instead actual JMA intensity scale is based on measured acceleration and velocity [19]. This observation bring doubt about the reliability of the JMA intensity scale as this index is the one used by majority of Japanese to evaluate the threat of an earthquake to humans living, and the intensity 7 recorded at MYG004 did not constitute any risk for citizen's life.

As previously mentioned, Motosaka also showed using short time length fourrier spectra and particle orbit analysis that partial uplifting of the seismometer concrete basement could have occurred at MYG004.

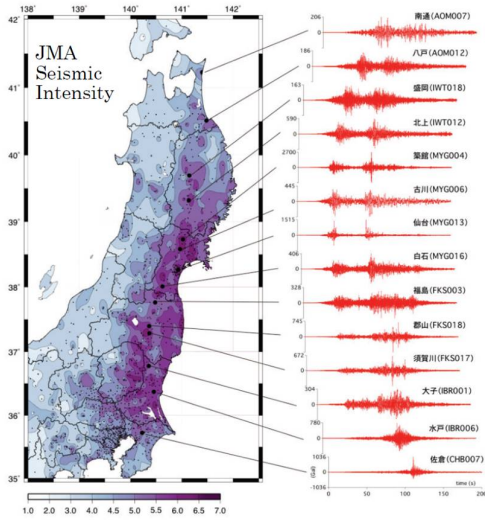

Figure 8: NS component of signal recorded along the Japanese coast [3]

Figure 9 show the ground motions characteristics as well as display that highlight the uptlift motions. Motosaka and Nagano [21] showed that partial uplift of the basement of a structure will provoke at the top level radiation of the horizontal predominant frequency on even multiplier for the vertical component and on odd multiplier for the horizontal components. Moreover the acceleration particle orbit of NS-UD plane show some strong specific orientation with one side half circle instead this motion should show elliptical shape.

2.4 Conclusion about ground motions study and linked structural damage observation

To conclude about previous study and structural damage observation in Tsukidate area, there is no agreement considering explanation of the low structural damage that were observed considering the high recorded ground motions at MYG004. It is reasonable to think that even if a partial uplifting had occurred a MYG004, the strong local site amplification that has been shown to occurred at this site is also a good indicator that suggest that the high intensity ground motions did not occurred on a very large area. Nevertheless the proximity of a undamaged wooden house (figure 4) is still problematic as it is not likely that less than 1500 gal took place as a ground solicitation to this house. Consequently it is still important matter to check the influence of high frequency content on high intensity ground shaking on the behavior of Japanese traditional constructions. To obtain such kind of low damage with high frequency and high acceleration signal could show that the method of calculation of the JMA intensity should be reconsidered.

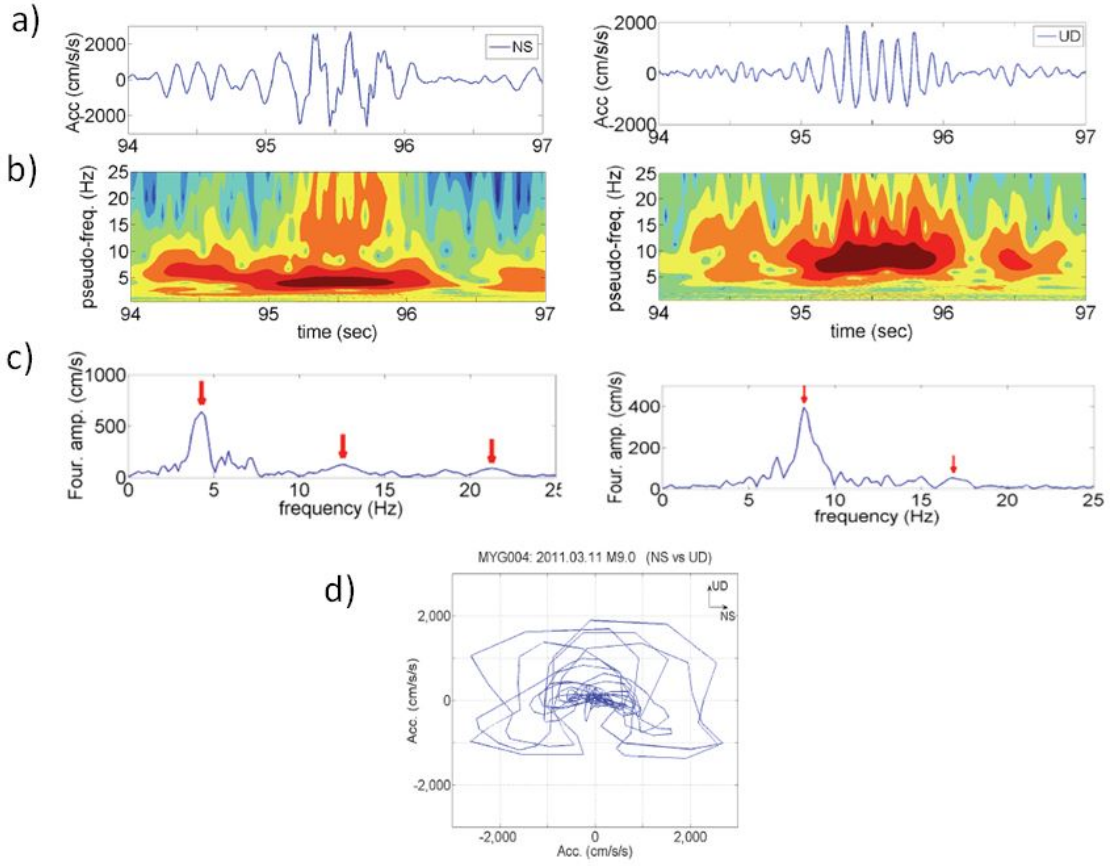

Figure 9: Characteristics of MYG004 ground motions at second peak: a) Acceleration data, b)Wavelet basis non-stationary spectra, c) Fourrier spectra, d) Acceleration particle orbit of NS-UD plane [3]

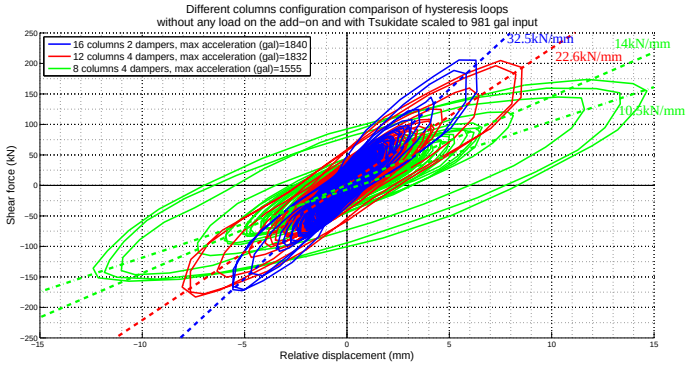

Figure 10: Hysteresis loops of the addon depending on the columns configuration

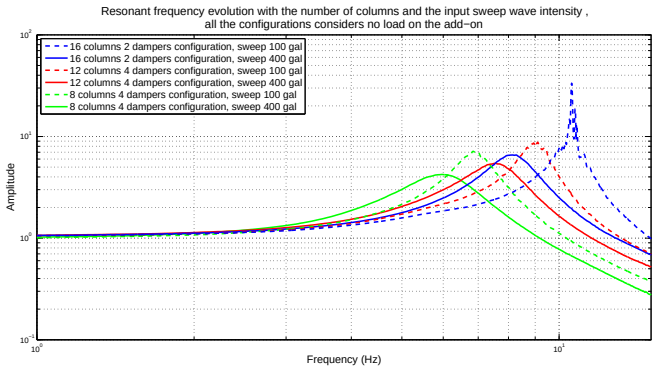

Figure 11: Spectral ratio of the addon structure depending on the columns configuration

3 Development of addon structure to amplify shake table acceleration

As introduced in the midterm report an addon structure was design to enable amplification of the shake table acceleration. This first addon design is shown Annex 1. Nevertheless the resonant frequency of this structure was not as low as planed and showed major amplification at 9 Hz instead the desired resonant frequency should have been close to 5 Hz. Consequently testings were performed in March intending to use the modularity of columns configuration to adjust the resonant frequency of the addon structure. Nevertheless the friction occurring at the connection level between the columns and the upper massive frame was still important so that, it lead to the creation of damage at connection level. Consequently a second design was created and will be presented in section 3.2.

3.1 Additional testing to the first design of the addon structure

The additional testing of the first addon design consisted in removing some of the columns to diminish the lateral stiffness of the addon, as well as studying the influence of additional load set on the upper frame and number of dampers installed on the structure. Consequently 16 columns, 12 columns and 8 columns configuration were tested and 1 and 3 tons as additional load were set on the upper frame. Figure 10 shows hysteresis loops of the different columns configuration. Moreover figure 11 displays the spectral ratio of the addon structure. It was decided to perform high acceleration sweep test to reduce the influence of the friction on the addon behavior. This influence of friction on the observed resonant frequency is shown figure 11. Instead 8 columns configuration could have provide the desired resonant frequency the resistance of columns for that configuration was no sufficient to be able to set additional mass on the top of the upper frame.

The friction occurring at the connection level lead to the damage initiation of the connected surface as it can be seen figure 13. This provoke blocking in one column connection that led to the overstress of that column at the bottom level and creation of a crack at the weld location (figure 12). Consequently the first design seems to be inappropriate as the strong friction taking place at the connection level endanger the addon behavior. As a result improvement of the addon structure was considered especially for the pieces that bring lateral stiffness to the upper frame.

Figure 12: Cracked welding at the bottom of one column

Figure 13: damaged columns due to friction occurrence

3.2 Improved design of the addon structure and its performance

Considering difficulties with the previous addon design, the improved design took special care of the connection that bring the lateral stiffness to the upper frame. As a result it was decided to provide lateral stiffness thanks to plates supported by rollers in order to diminish the possibilities of friction occurrence. Besides to reduce the tuned mass damper discussed in the midterm report, only half of the massive upper frame was considered. Indeed tuned mass damper effect should be proportional to the mass ratio between the addon structure and the shake table. Consequently the mass of the upper frame of the improved addon will be about 5 tons. To provide the desired resonant frequency as well as guaranteeing the maximum loading strength, it was decided to use super Duralumin plate which enable to have important yielding strength as well as an important ductility. The characteristic of the duralumin plate are as follow: 75 Gpa as Young modulus and 510 Mpa as yielding strength. The possibility to fit both needed maximum shear strength as well as needed resonant frequency would have been much more complex using regular steel.

Design process was performed using FEM model developed using CAST3M. The mechanical plan of the improved design is shown figure 14. This plan shows the presence of the plates on both side of the upper massive frame that at supported by 8 columns on which rollers are set. The vertical support of the massive frame is also provided by columns that use rollers on their top. Hence the lateral stiffness is only provided by the duralumin plate and sources of friction should be strongly reduced. Using FEM model the first vibrating mode that was planned to be 6.5 Hz was overestimated to 7.1 Hz. This first mode shape and its related stress considering 1 m maximum displacement is shown figure 15. The overestimation of the resonant frequency compared to theoretical calculation could be due to the stress localization at the connection level due to sharp edge of the connection. Indeed using FEM model simplified connections are considered as the bolted connection is not represent and this connection should regularize the stress at the connecting parts boundaries. For this FEM model the columns supporting the plate which gives lateral stiffness to the addon were not modeled and considered as pin contact to the plate.

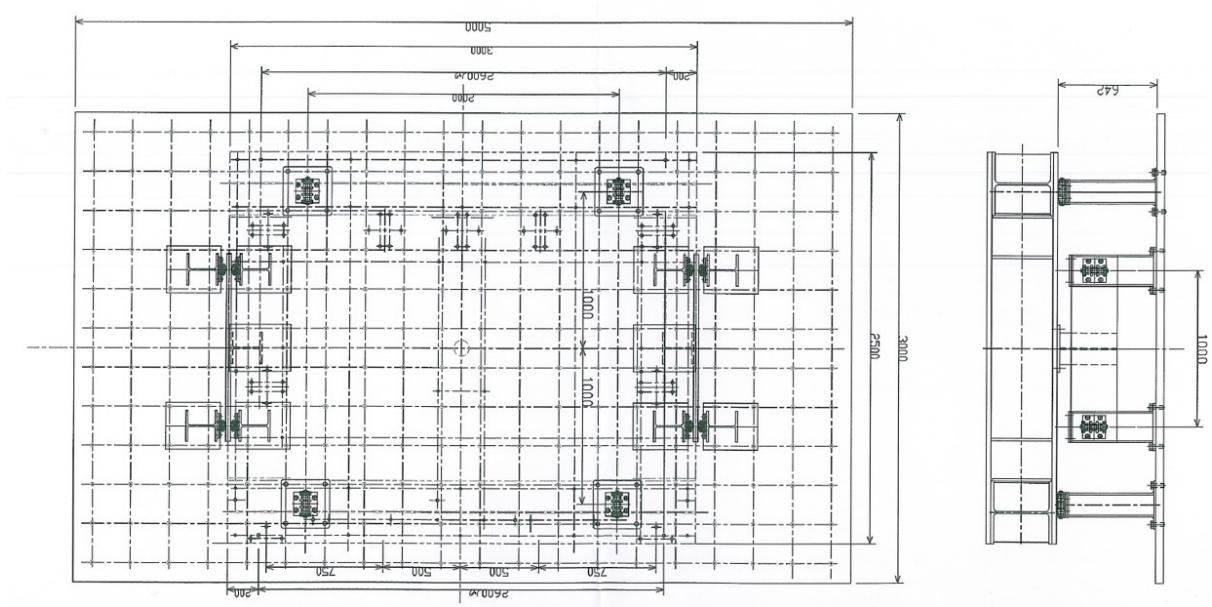

Figure 14: Plan of the improved design of the addon structure

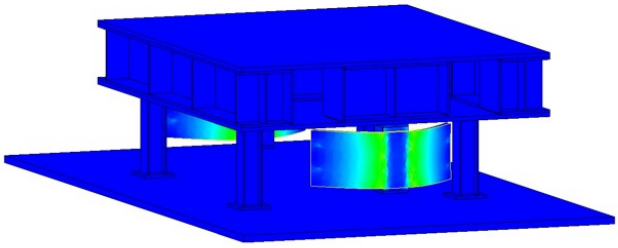

Figure 15: Shape of the first vibration mode and its related stress distribution considering 1 m maximum displacement

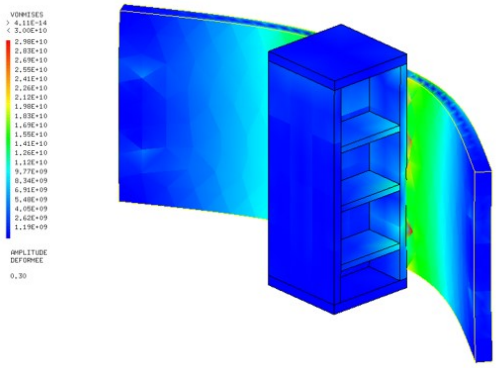

Figure 16: Stress localization at the connection level

The performance of the improved addon structure was evaluated by testing different configurations. First, the characteristics of the super Duralumin plate was tested by quasi-static test. Secondly the addon without any load on it and with 2 dampers was tested using sweep wave (sweep 1-20 Hz 400 gal maximum acceleration) as well as with Tsukidate scaled to 1g input. Then 2 tons load was set on the upper massive frame and finally the 2 dampers were removed. Figure 17 to 22 show hysteresis loops recorded during these tests as well as spectral characteristics of the improved addon design. It is seen on hysteresis loops that the behavior of the addon has been notably improved. Moreover the maximum acceleration reached on the top of the upper frame reached 2900 gal when 2 tons where set on the addon and the 2 dampers were removed. Despite the strong improvements some nonlinearties occurred when acceleration higher than 2300 gal was reached. These nonlinearities were mainly due to some uplift of the massive upper frame. Indeed as it can be seen on mechanical plan figure 14, during the design process the overturning moment that could occur was not remarkably considered and only parts to prevent the partial uplift consisting in plates set on the top of column that support lateral plates were installed.

In addition despite the diminution of the total weight of the addon, strong damping occurred on the shake table motion as it can be seen on figure 20 to 22. This tuned mass damper system can be then analyze as difficulties of the servo-valve controller system that command the shake table motion to make actuator act as rigid boundaries when force is transmitted to the upper frame. This behavior is also explain by the setting of this experiment where an important shear force is transmitted thanks to high stiffness parts to a low rise heavy upper frame. The spectral ratio of the addon experiment also show that the peak shape of MYG004 ground motion can be quite well reproduce even when the maximum acceleration on the top of the addon is not so high. For instance when the addon was tested without any load on the top of it and with 2 dampers, as it can be seen on figure 20 the frequency content of MYG004 signal is correctly reproduce from 4 Hz to 7 Hz even if the maximum acceleration on the top of the addon is only 1700 gal. Futhermore the overestimation of the first vibrating mode using FEM software was confirmed since desired resonant frequency of about 6 Hz for the addon without any load and 5 Hz for the addon with 2 tons load was obtained. However tuned mass damper effect is lowering maximum amplified frequency. In fact, if the spectral amplification is considered as being the ratio between top of the addon acceleration spectra and the input command spectra instead of using the shaking table acceleration spectra, then the amplification spectra is shifted to lower frequency and widened. This effect is shown on figure 20 to 22 considering effective amplification.

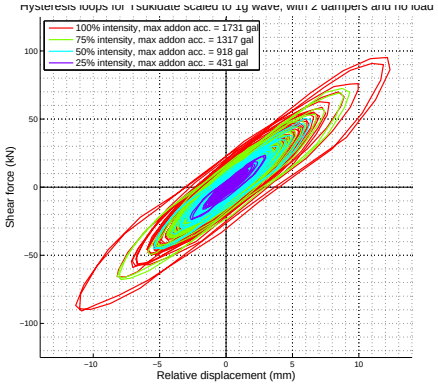

Figure 17: Hysteresis loops without load, 2 dampers

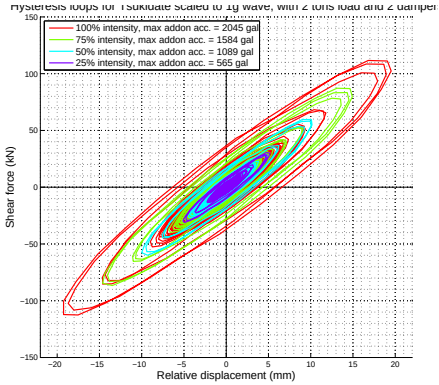

Figure 18: Hysteresis loops 2 tons, 2 dampers

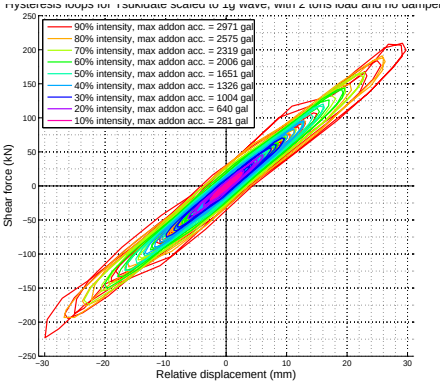

Figure 19: Hysteresis loops 2 tons, 2 dampers

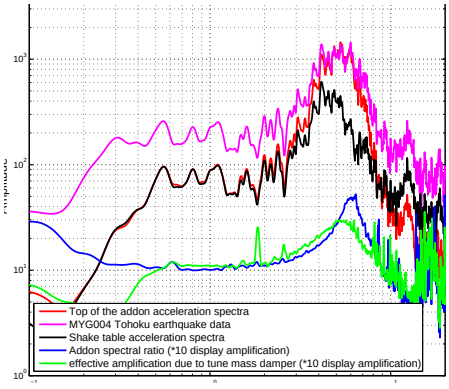

Figure 20: Spectral characteristics no load, 2 dampers

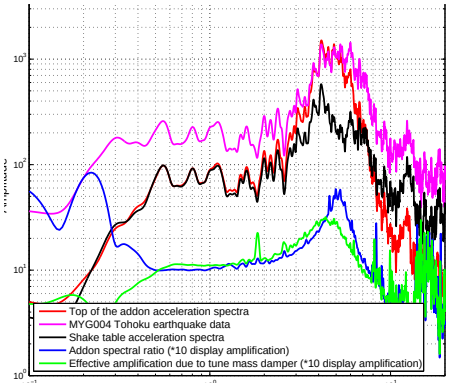

Figure 21: Spectral characteristics 2 tons, 2 dampers

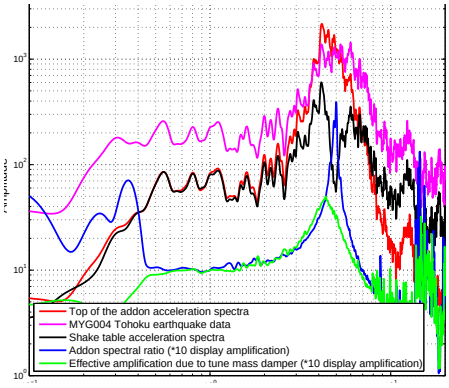

Figure 22: Spectral characteristics 2 tons, no dampers

4 Wood frame structural experiment

As the addon showed satisfying linear behavior as well as high amplification for the configuration without dampers, it was decided to keep this configuration to set the wood frame on its top. The testing consisted in using one wood frame with traditional Japanese construction techniques and apply different reinforcement techniques on it. The mechanical plan representing the wood frame with wall of columns type of reinforcement is shown figure 23. The principle of this reinforcement will be presented in following section. The frame consisted in eight beams that are loosely connected to the lower and upper beams. Indeed holes in the beams are designed to be 1 cm larger than the column connections part as shown figure 25. Moreover a pullout prevention system is installed on the bottom and top of the outer columns and connected to the beams to avert the column to be disconnected from the beams. The beams are connected together by steel plates that only have low participation to the wood frame resistance and stiffness.

Figure 24 shows different reinforcement techniques applied to the wood frame. Braces and panels correspond to classical reinforcement applied to majority of Japanese houses instead wall of columns solution is a newly developed technique. The configurations showed figure 24 were tested using Tsukidate signal scaled to 1g PGA as input signal, and in addition wall of columns configuration was also tested using JMA Kobe input recorded during 1995 Great Hanshin earthquake. It was intended to compare the wood frame behavior depending, on the frequency content of the input signal (see figure 2), as well as between a signal that correspond to uncommon high acceleration with low damage occurrence (MYG004) with an input signal that correspond to highly damageable to structure ground motions (JMA Kobe). JMA Kobe signal have maximum acceleration of 820 cm/s^2 with a predominant frequency about 1 Hz. Furthermore these different reinforcement techniques were previously tested during a different experimental campaign using JMA Kobe signal on the same frame. Nevertheless during these tests only one side reinforcement was applied without any additional braces as shown figure 26. From these results, the braces behavior and the wall of columns behavior will be detailed in the next section. The panels behavior will not be discussed as it was close to the braces behavior and the loading pattern with Tsukidate input was stopped after 60% intensity test. During those tests to consider the influence of a second floor and the roof, 2 tons additional mass was set on the upper platform of the wood frame. The total weight of the structure considering the additional weight is about 2.5 tons.

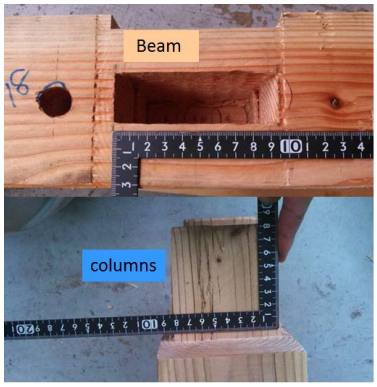

Figure 25: Loose connection between the beam and the columns

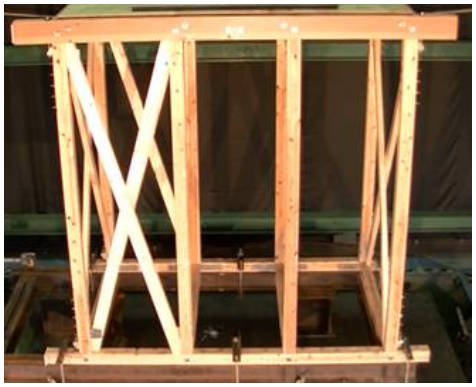

Figure 26: One side reinforcement tested with JMA Kobe signal

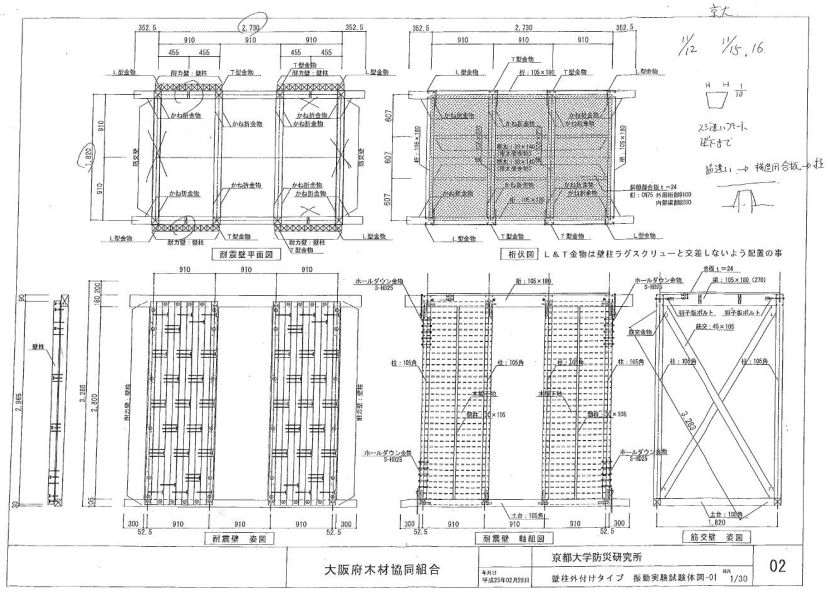

Figure 23: Mechanical plan of the wood frame with wall of column reinforcement

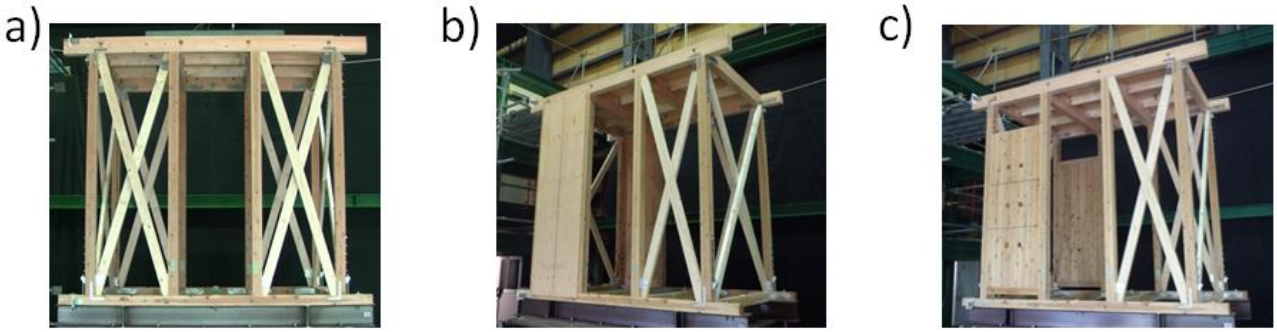

Figure 24: Different reinforcements applied to the woodframe. a) Braces reinforcement. b) Panels reinforcement. c) Wall of columns reinforcement

4.1 Braces reinforcement behavior

The braces reinforcement correspond to diagonal wood beams that are installed on side openings of the wood frame. These are installed with a small clearance about 1 mm and then connected with screws to the columns thanks to low resistance aluminium plates. Despite the connecting plate have a low resistance the failure of brace system commonly occurs as the 2 braces in compression suffer from important buckling participation to their loading and can fail on their middle going out of the loading plane, automatically after the screws of the 2 braces in tension can be a pulled out from the columns. This failure process is characteristic of the braces system and occurred for JMA Kobe input for 80% intensity (771 gal maximum acceleration). The specimen state just after the braces failure considering JMA Kobe input test is shown figure 30.

The experimental set up used for Tsukidate ground motions input simply differs from using the addon structure, and braces were installed on both side openings of the wood frame. Despite no damaged occurred on braces even with an acceleration input on the bottom of the wooden frame of 1427 gal using Tsukidate ground motions, the loading pattern had to be stopped due to the tightness of the pullout prevention system. In the case of the pullout prevention system to get too tight, it can provoke the failure of the frame consisting in one of the extreme part of the bottom beam to break. The cause of this pullout system to get tight cannot be totally related to the wood frame behavior and could be due to the addon undesirable rocking motion. For 80 % intenstity of Tsukidate ground motion, the maximum rocking displacement that occured on the top of the addon was 1 mm.

Nevertheless the study of the hysteresis loops figure 27 and 28, of recorded acceleration spectra figure 29 and acceleration time histories figure 31, still clearly show influence of the input signal on the wood frame behavior. The guessed location of braces failure for JMA Kobe input correspond to the following characteristics of loading on the frame: shear force 16 kN and relative displacement 56 mm (see figure 27). Considering Tsukidate input signal and the difference of the specimen configuration half of the shear force can be heed. Therefore the loading on the braces seems to be much lower even for Tsukidate input with 1427 gal maximum acceleration on the top of the addon. This method of considering only half of the shear force can be seen as imprecise and further testing using the same structure as the one for Tsukidate ground motions solicitation may be needed. Nevertheless the difference of loading can be also analyze as the low amplification that is observed figure 29 at the second peak of Tsukidate ground motions (75 s to 85 s). Indeed amplification of the input signal is only observed on a narrow high frequency band from 2 Hz to 4 Hz which does not correspond to high inputed frequency. On the contrary with JMA Kobe input amplification of the ground motions spectra is observed in a frequency band from 0.5 Hz to 1.5 Hz which correpond to predominant frequency of the ground motion. This effect is also notable on acceleration time histories (see figure 31 as for JMA kobe the acceleration on the top of the wood frame is about 1.3 times higher than the input at the moment of the braces failure instead for Tsukidate input the acceleration on the top of the wood frame is remarkably lower than the input.

To conclude about the braces behavior, it was clearly observed that the frequency content of Tsukidate ground motions is lowering the possibilities of damage initiation on the frame due to the non amplification of Tsukidate ground motions in the frequency range between 4 Hz and 7 Hz. In addition the acceleration spectra on the top of the wood frame for Tsukidate input is much lower in the frequency range from 0.5 Hz to 1.5 Hz than for JMA Kobe input, so consequently with Tsukidate input no strong relative velocity and relative displacement are created on the top of the wood frame even for high intensity input. It is therefore shown that relative velocity and displacement must have a primordial impact on the damage initiation on the wood frame.

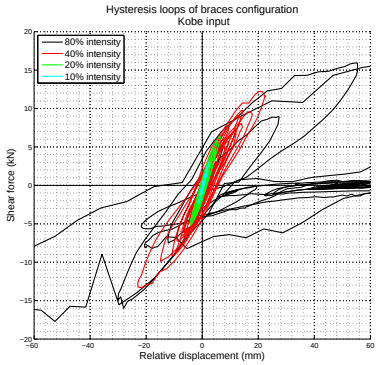

Figure 27: Hysteresis loops of braces configuration with Kobe input

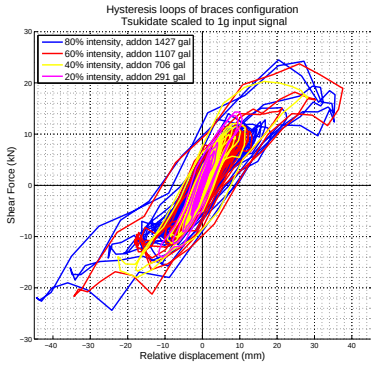

Figure 28: Hysteresis loops of braces configuration with Tsukidate input

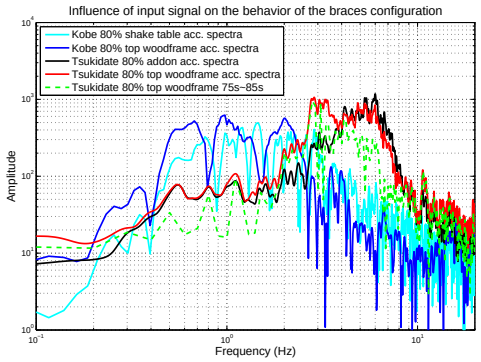

Figure 29: Comparison of spectral wood frame behavior for braces reinforcement.

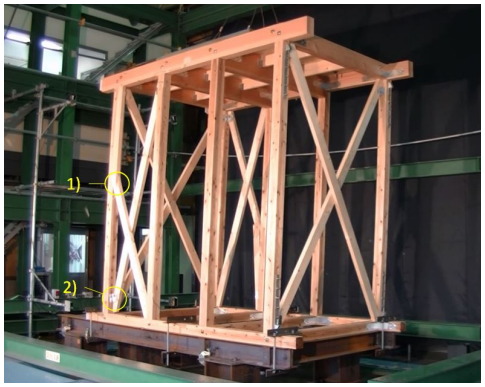

Figure 30: Braces reinforcement specimen used with JMA Kobe input. 1) Compressed brace failure. 2) Screws of the connecting plate pulled out from the column

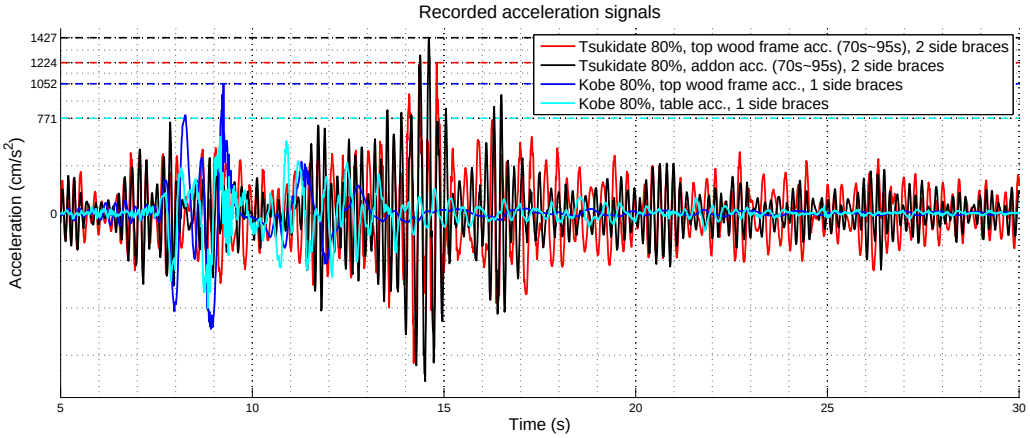

Figure 31: Time comparison depending on input for braces configuration

4.2 Wall of columns reinforcement behavior

The wall of columns system is a newly developed reinforcement techniques that is installed in few Japanese wooden houses. This reinforcement, shown figure 32, consists in columns that are bolted together, an additional bottom beam nailed to the wood frame columns is maintaining vertically the columns used for reinforcement. This system is intending to bring lateral stiffness to the wood frame as well as providing important energy dissipation thanks to the columns friction when relative displacement is large. The wall of columns reinforcement show notable improvement of the wood frame capacity to resist to JMA Kobe input as the wood frame configuration shown figure 34 only failed for JMA Kobe 120 % intensity input which correspond to a maximum acceleration of about 1 g. Compared to the other reinforcement that are used, the wall of columns show some specificity when failure occurs. Indeed when too large loading is reached, instead of having the reinforcement technique that fail it is likely that the reinforcement will still have enough loading capacity and will transmit an important part of the force to the frame that will fail. This was observed for that structure with JMA Kobe input for 120% intensity. The hysteresis loops obtained with such a configuration and considering JMA Kobe input are shown figure 33.

The behavior of the wall of columns system is showing two different kind of nonlinearities depending on the maximum input. For relatively low input, until 80 % intensity of JMA Kobe ground motions, The behavior of the wood frame is bi-linear with a quite stable increase of the hysteresis loops. For JMA Kobe 80% a different nonlinear behavior is observed with a progressive increase of the stiffness as the relative displacement increase. In addition for this range of relative displacement (higher than 50 mm), the unloading progressively show some specificity with a decrease of the shear force with a stiffness close to the initial one followed by a decrease of the relative displacement with a stiffness close to zero. This behavior also show a decrease of the energy dissipation over one loading cycle. This distinct nonlinear behavior can be analyze as the effect of the columns bolt hole to get enlarged during large displacement motions. After this large relative displacement is reached the unloading stiffness comes from the columns friction and then is almost none as the columns are back to their initial position and the bolts does not tight the columns together anymore.

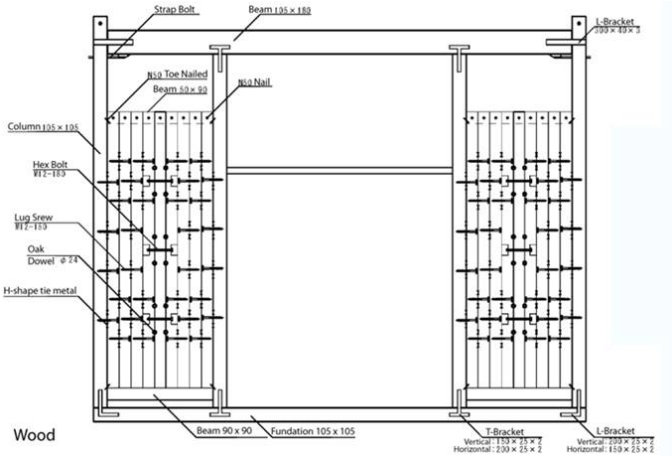

Figure 32: Wall of columns reinforcement

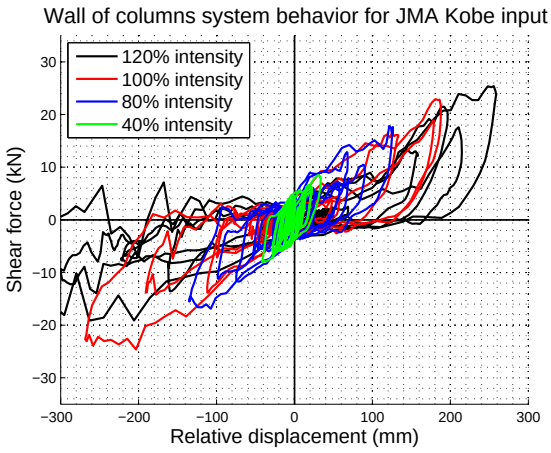

Figure 33: Hysteresis of wall of columns configuration for JMA Kobe input

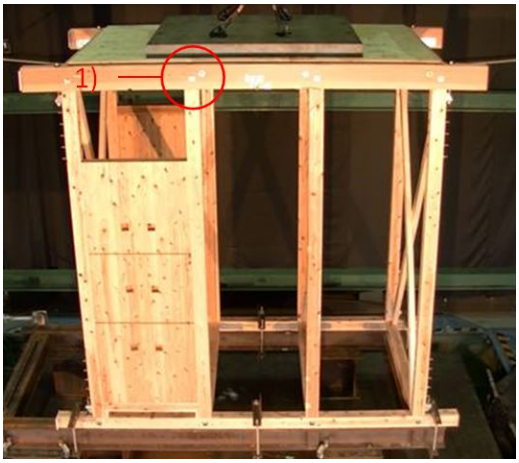

Figure 34: Wall of columns specimen tested with Kobe input without side braces. 1) location of failure for 120 % intensity

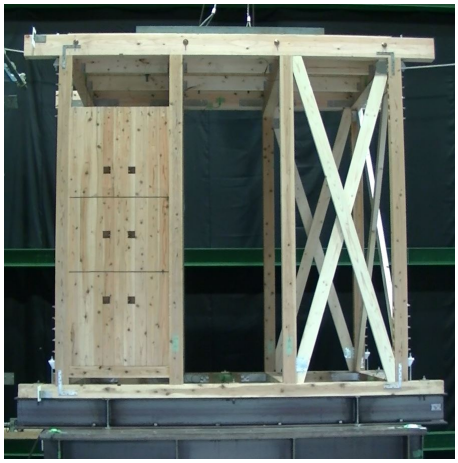

Figure 35: Wall of columns specimen tested with Tsukidate input

As the wall of columns reinforcement is a newly developed techniques some way to improve it was tested. Consequently two different specimen configurations were used with Tsukidate input. Both these configurations used braces on the other side openings as shown figure 35, however after first testing pattern, double sided tape was installed between each columns of the of the wall of columns. Using double sided tape, it was intended to bring additional dissipation to the structure. The regular configuration hysteresis loops are shown figure 36, it is observed that this configuration show quite same bi-linear behavior as observed with JMA Kobe input without any braces on the other side. The wall of columns using double sided tape showed quite different behavior especially for low input as displayed figure 38. Nonetheless this difference is no longer observed when signal higher than Tsukidate 40% is used. The low influence of the tape on the wall of column behavior is shown figure 37. As a result for the further development the influence of the tape will not be considered. As shown figure 31 even for strong maximum acceleration (1400 gal as PGA) on the top of the addon the behavior of the wall of columns system stay bi-linear and no additional nonlinearities are

observed. Moreover created relative displacement is still quite low and it is likely that higher intensity could have been used without damaging the structure.

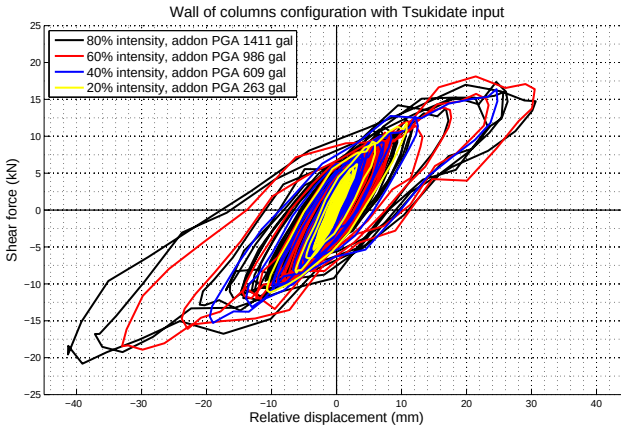

Figure 36: Hysteresis loops for regular configuration of wall of columns system

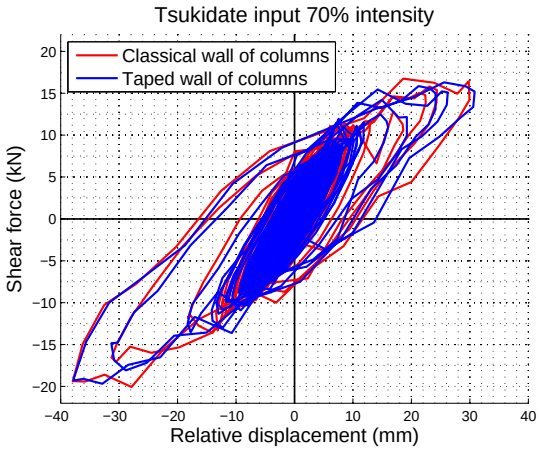

Figure 37: Comparison of wall of columns and taped wall of columns configuration

Besides testing using Tsukidate input signal, JMA Kobe signal was used on the similar structure. Therefore addon structure was removed. The observed hysteresis loops during these testing is shown figure 39. It shows some interesting influence of the presence of braces and tape to the structure behavior. The specific nonlinearity observed for previous testing using JMA Kobe, with progressive increase of the stiffness when relative displacement larger than 50 mm is reached, is not as strong as previously. Especially the low stiffness observed during unloading process is no longer observed. This behavior must be due to the presence of braces on one side as both these systems have an opposite nonlinear behavior, for the wall of columns system the nonlinear behavior consist in a progressive increase of the stiffness instead the braces system show about 10% of the initial stiffness when large relative displacement are reached. This reinforcement show then interested behavior as it prevents the creation of high shear force on the structure. For 120 % intensity of JMA Kobe, the failure of the structure did not occurred. Nonetheless some important damage on the brace that were cracked at the connections and bottom beam of the wall of columns was pulled down from about 1 cm. The damage observation performed after this test are shown annex 6 . In addition same comparison of acceleration spectra and acceleration time histories can be performed depending on used signal input. This study is shown figure 40 and figure 41. The same amplification characteristics than for the braces reinforcement is observed. For JMA Kobe input the top of the wood frame maximum acceleration is about twice of the maximum input acceleration. On the contrary for Tsukidate input despite the maximum input acceleration is as much as 1411 gal, the top of the wood frame maximum acceleration is only about 1000 gal, so lower than the input. This effect is observed on the acceleration spectra figure 38 due to the low amplification at the Tsukidate second peak acceleration from 75 s to 85 s. On the contrary, for JMA Kobe input the amplification of the input signal due to the structure behavior is occurring at the predominant frequency of the ground motions. Moreover since this amplification is occurring for lower frequency, important relative velocity and relative displacement is reached on the structure.

To conclude about the wall of columns behavior, important capacity to resist to Tsukidate ground motions have been observed. It is likely that this reinforcement could have endure more than 2000 gal as maximum solicitation due to the low created acceleration on the top of the wood frame and relative displacement. It

then may be needed to perform the same test, using Tsukidate input, on one wood frame that will be led to its failure. To preform such a test the addon behavior may had to be improved.

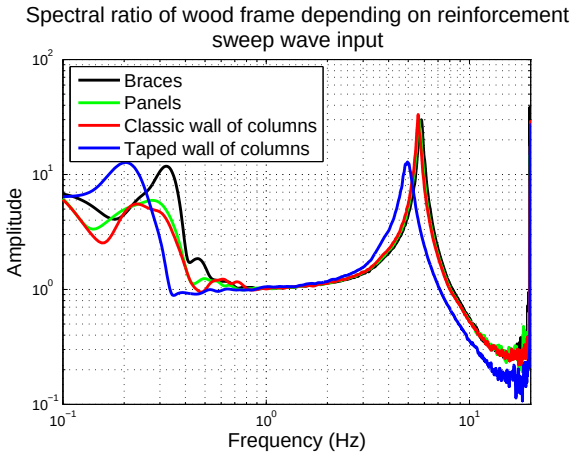

Figure 38: Different reinforcements spectral ratio

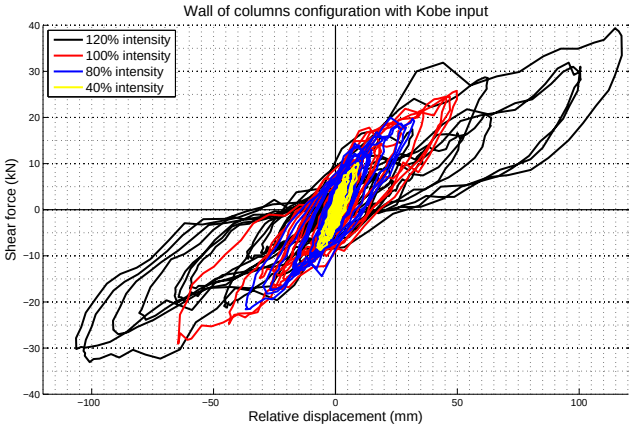

Figure 39: Wall of columns with brace reinforcement behavior for JMA Kobe input

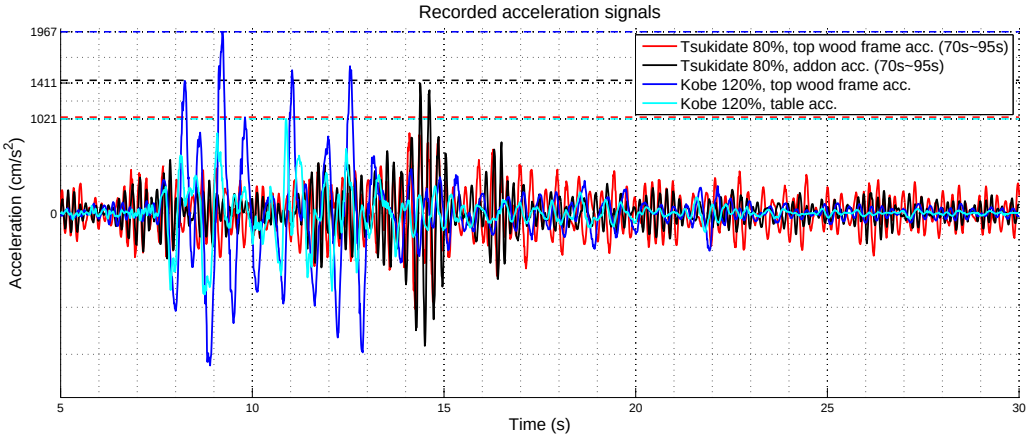

Figure 40: Comparison of acceleration time history depending on input with wall of columns configuration

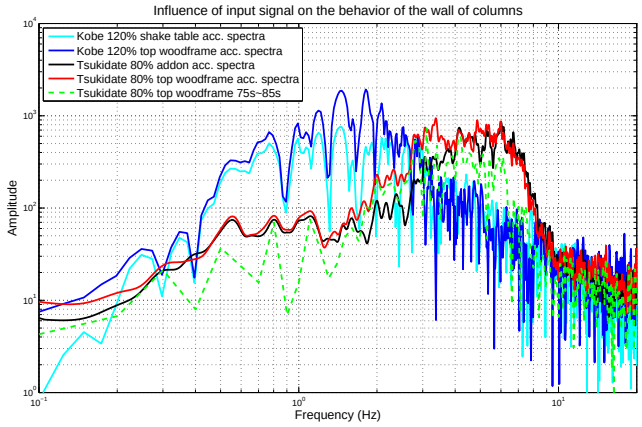

Figure 41: Comparison of acceleration spectra depending on input signal with wall of columns configuration

4.3 Addon behavior during wood frame experiment

Important observations were performed for the addon behavior when wood frame was installed on its top. The influence of the wood frame to the addon behavior lowered notably the amplification of the ground motions input obtained with the use of the addon for low intensity shake table input. Tuned mass damper that was previously observed on the shaking table also did not occurred as remarkably. This is shown figure 42 by observing acceleration spectra recorded on the shaking table for the different experiment configurations. Indeed tuned damper system behavior was observed between the wood frame and the addon especially for low input signal such as for the sweep input wave and Tsukidate 10% intensity input. This effect is occurring since resonant frequency of the wood frame structure is near the one of the addon and the mass ratio between the two structures is about 0.5. The spectral ratio of each structure obtained during sweep wave tests is shown figure 43. Its observed a low amplification of the addon at the resonant frequency of the wood frame. Nonetheless due to the important nonlinearity occurring on the wood frame for larger input, the tuned mass

damper behavior is no longer observed for larger input due to the resonant frequency shift of the wood frame induced by its nonlinearities.

This specific behavior need to be studied to be able to predict the addon spectral characteristics for further experiment. As a consequence numerical model of the experiment stages were created.

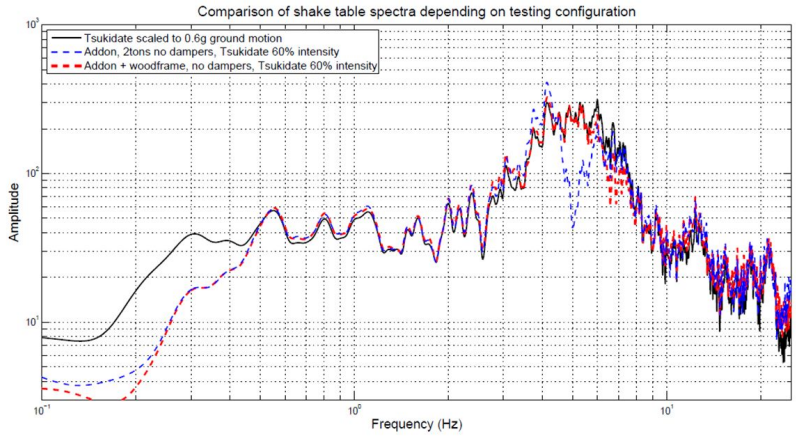

Figure 42: Comparison of shake table acceleration spectra depending on testing configuration

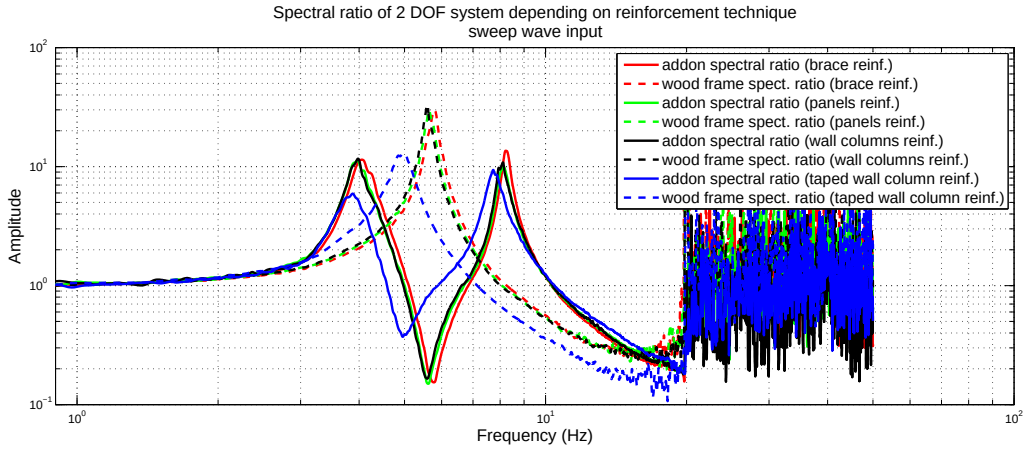

Figure 43: Spectral ratio of the wood frame and the addon depending on reinforcement technique

5 Numerical simulation of the addon behavior

In order to analyze in detail the addon behavior and be able to evaluate its physical parameters different numerical model of the experiments were used.

Spring-mass system for 1 degree of freedom oscillator

Initially spring-mass model of one degree of freedom oscillator was created. This model intend to reproduce the addon behavior, when the addon only was tested. It uses Newmark algorithm to numerically calculate the motions. The used input signals were the recorded acceleration on the shaking table so that influence of the tuned mass damping system occurring on the shaking is avoided. The respective obtained spectral ratio and hysteresis loops are displayed figure 44. This model uses same stiffness for both no load 2 dampers and 2 tons 2 dampers configurations with a value of 8e6 N/m. This value had to be tuned for the 2 tons and no dampers configuration with a value of stiffness of 7.2e6 N/m. This need of tuning is explained by the participation of dampers to the stiffness. To obtain such a result it was decided to focus on the reproduce spectral ratio. Indeed despite the similarity of reproduced spectral ratio the hysteresis loops show some important difference. Notably some damping mechanism which is not seen on the spectral ratio is seen on hysteresis loops. Nevertheless the maximum acceleration and relative displacement of each wave are correctly reproduced.

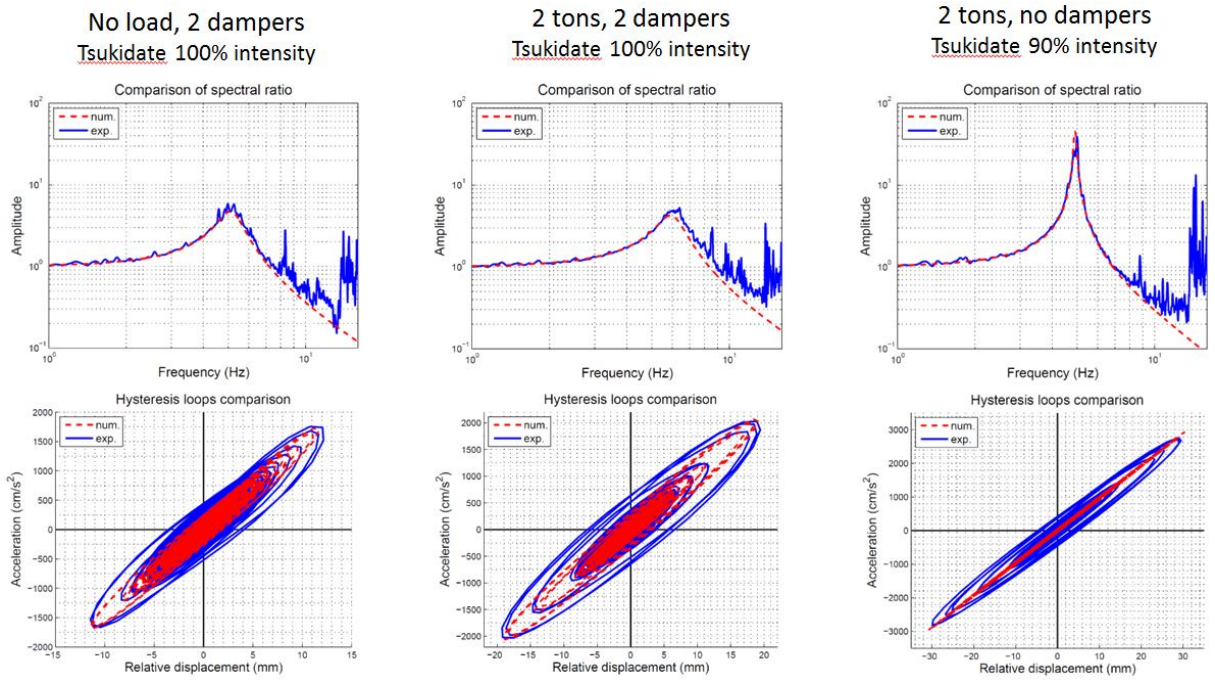

Figure 44: Spectral ratio and hysteresis loop of simulated sping-mass system

FEM simulation of the addon testing

Due to the lack of damping on observed simulated hysteresis loops, it was decided to use FEM model to perform same simulation. This model need some tuning though because of the stress concentration discussed part 3.2. Consequently the distance between the pin contact on the plate was progressively increased until

the hysteresis loops show corresponding slope with experimental data. Same method was used to reproduce the influence of dampers. The reproduce spectral ratio and hysteresis loops are shown figure 45. The spectral ratio appears to have some non stability for frequencies higher than 7 Hz. This specific behavior is provoked by some weakness of the used mesh so that pin contact points are not perfectly symmetric. This weakness is also observed for the 2 additional tons and no damper configuration, for which tuning could not be as fine as desired and reproduced stiffness is larger than experimental one. Nonetheless the same special damping mechanism is observed on hysteresis loops so that consistence with spring-mass model is observed.

As a consequence, the special lack of damping observed on hysteresis loops must be due to some experimental problem and further study of the experimental data need to be done. The additional load set on the FEM model, that keep the same distance between pin contact, enable to calculate apparent stiffness and vibrating mass of the model. As a result comparison with spring-mass model show difference of stiffness and vibrating mass of less than 3%.

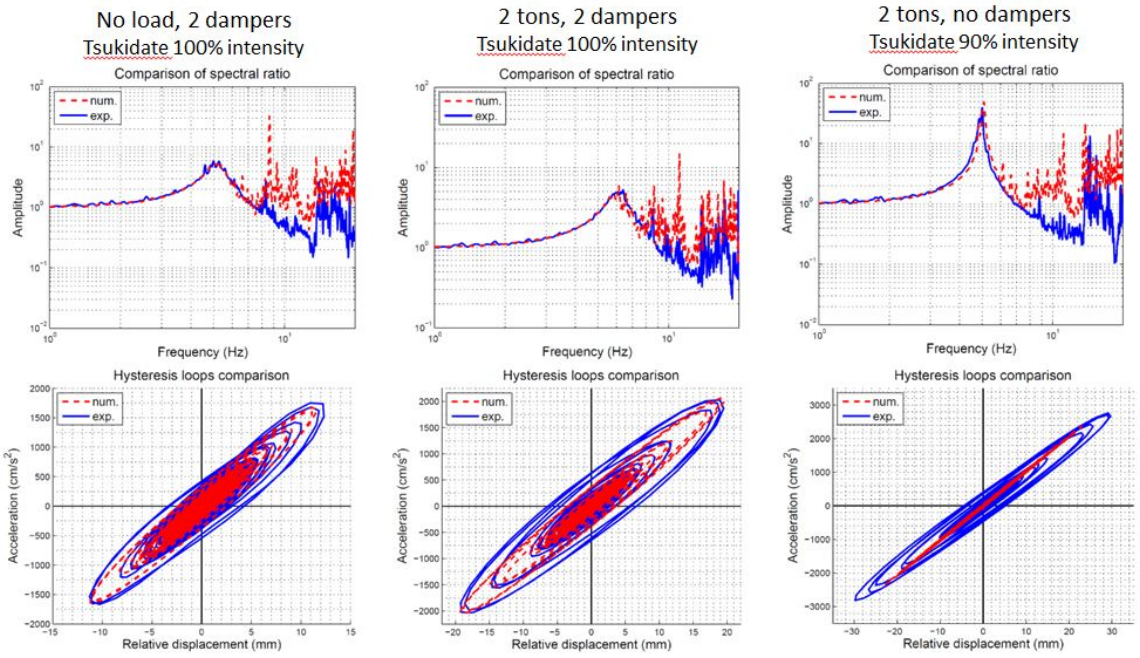

Figure 45: Spectral ratio and hysteresis loop of simulated FEM model

Spring-mass system for 2 degree of freedom oscillator

In order to study experimentally observed tuned mass damper system, the wood frame behavior was added to previous spring-mass model. The tuned mass damper behavior correspond to equation 1 which parameters are expressed figure 46. The wood frame characteristics was calibrated using spring-mass system of the wood frame only and using recorded addon acceleration as input to the model. This enable to evaluate stiffness, mass and damping of the wood structure.

$$\begin{pmatrix} M_p & 0 \\ 0 & M_w \end{pmatrix} \begin{pmatrix} \ddot{v_p} \\ \ddot{v_w} \end{pmatrix} + \begin{pmatrix} C_p + C_w & -C_w \\ -C_w & C_w \end{pmatrix} \begin{pmatrix} \dot{v_p} \\ \dot{v_w} \end{pmatrix} + \begin{pmatrix} K_p + K_w & -K_w \\ -K_w & K_w \end{pmatrix} \begin{pmatrix} v_p \\ v_w \end{pmatrix} = - \begin{pmatrix} M_p \\ M_w \end{pmatrix} \ddot{u} \qquad (1)$$

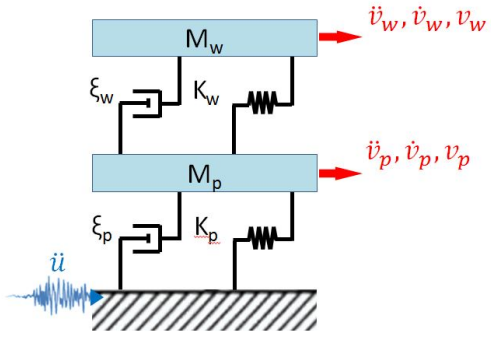

Figure 46: Representation spring-mass sytem for 2 degree of freedom oscillator evaluation

The wood frame show important nonlinearity when Tsukidate input higher than 20% intensity is used. As a result the spring-mass model was only used with sweep wave and Tsukidate 10% intensity as input. The simulated spring-mass model show good correspondence for both input considering the spectral ratio (see figure 47 and figure 48) . Nevertheless the same lack of damping in hysteresis loops is observed on numerical result (see figure 49 to figure 52. In addition for Tsukidate 10% intenstity nonlinearity is observed on the woodframe at the second peak so that hysteresis loop shows some difference of slope.

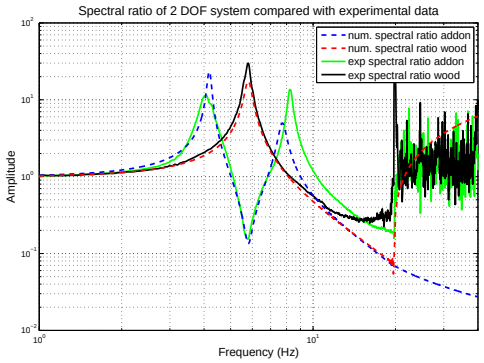

Figure 47: Simulated spectral characteristics for the spring-mass system with Tsukidate 10% intensity

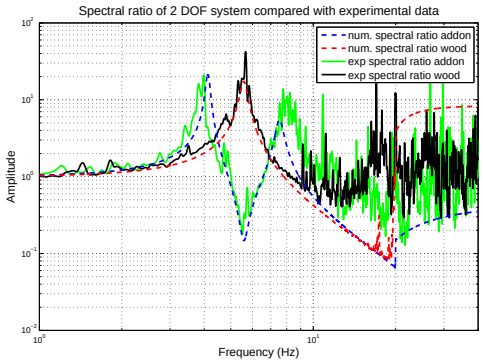

Figure 48: Simulated spectral characteristics for the spring-mass system with sweep wave

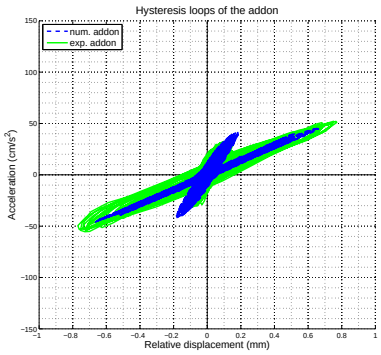

Figure 49: Hysteresis loops of the addon for the spring-mass system with Tsukidate 10% intensity

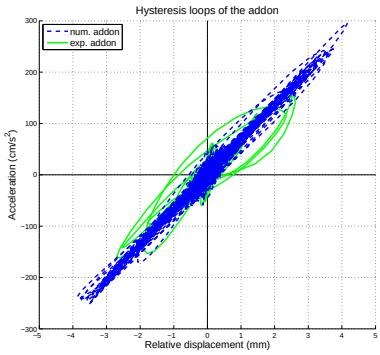

Figure 50: Hysteresis loops of the addon for the spring-mass system with sweep wave

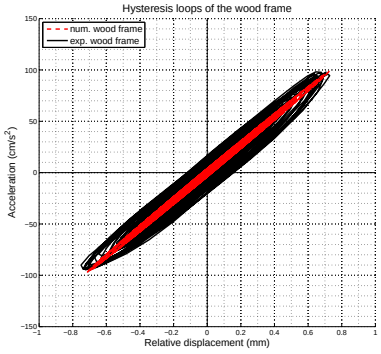

Figure 51: Hysteresis loops of the wood frame for the spring-mass system with Tsukidate 10% intensity

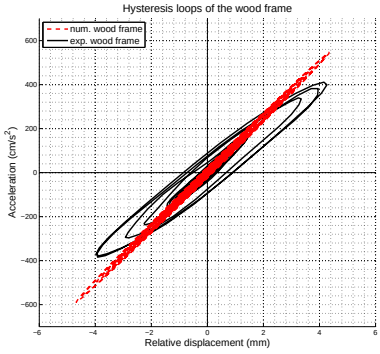

Figure 52: Hysteresis loops of the wood frame for the spring-mass system with sweep wave

FEM model for addon with wood frame experiment

As FEM model was calibrated, it was also intend to reproduce the addon behavior for the testing using wood frame on the top of the addon. Due to the difficulties to charaterize the wood frame connections and the important clearance between several parts, the creation of FEM model of the wood frame is difficult. Therefore, the influence of the wood frame to the addon was simulated using a beam element reproducing same force-displacement relation and mass of the wood frame. The mesh of this model representing first vibration mode is shown figure 53.

This model showed ability to successfully find vibrating properties of the system without any further tuning for the addon behavior. The simulation were only performed using Tsukidate 10% intensity wave, due to the low quality of the shaking table displacement data for sweep wave displacement range. The spectral ratio of the structure using FEM model is correctly reproduced as shown figure 53. As for previous models lack of damping is observed on hysteresis loops (see figure 54 and 55).

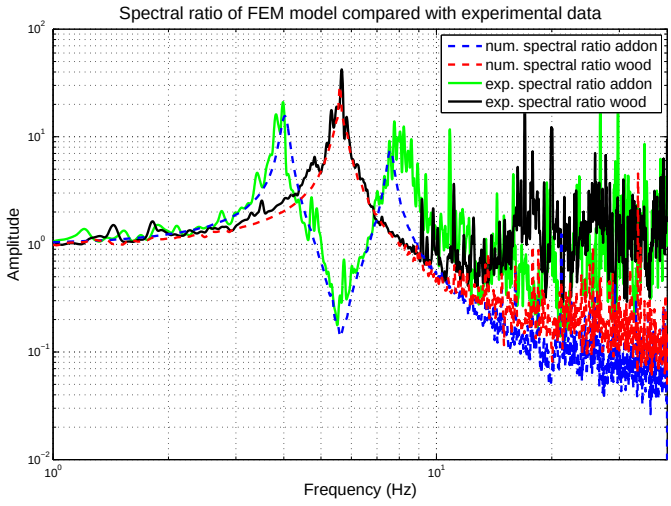

Figure 53: Simulated spectral characteristics of the addon and woodframe system with FEM model

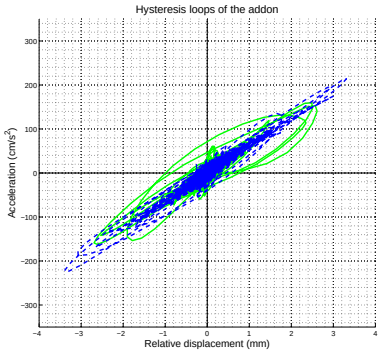

Figure 54: Hysteresis loops of the addon structure with FEM model

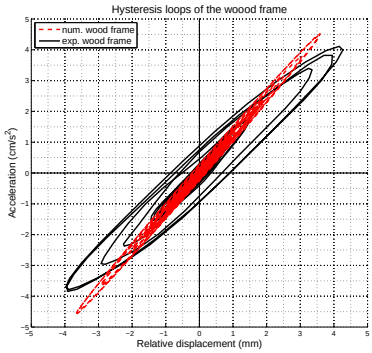

Figure 55: Hysteresis loops of the wood frame structure with FEM model

Conclusion about created numerical models

As a conclusion two different numerical models were created and calibrated in order to reproduce the observed behavior of the addon structure. These models show satisfying capacity to reproduce the spectral characteristics of every different configurations. It also highlight a need of further interest into the experimental data due to the specific damping mechanism that is only seen on hysteresis loops. As a consequence spectral ratio and hysteresis loops of other directions should be observed in order to find a specific behavior that was not already found in previous analysis.

The use of spring mass system as well as FEM models show some good complementary qualities as FEM model provide a lot more information about the structure behavior but also have a more important computational cost.

Moreover to enable an advanced study of the evolution of the tuned mass damper system behavior with the increase of Tsukidate input intensity, a nonlinear model for the wood frame could be implemented. This nonlinear behavior was already created considering the braces reinforcement and it consists in a tri-linear elastic behavior. Figure 56 shows the implemented tri-linear behavior on a spring-mass model solved with Newmark algorithm. This nonlinear model showed good capacity to represent the wood frame behavior for Tsukidate input motion of intensity higher than 40%. In addition the nonlinear relation between the lateral force and the displacement could be implemented on the beam used in the FEM model.

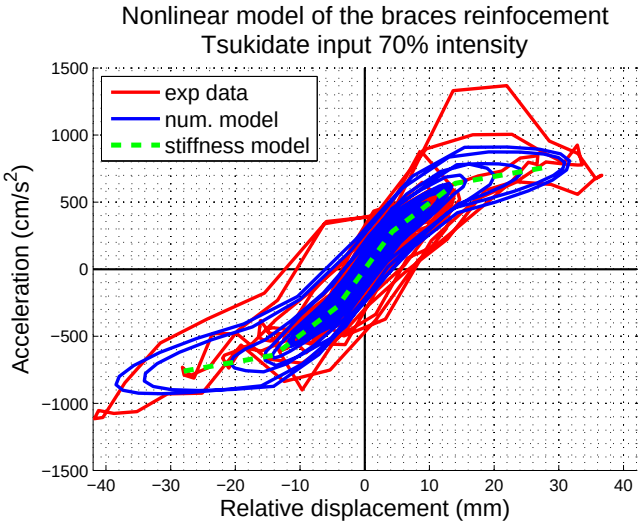

Figure 56: Simulated nonlinear behavior of the wood frame with braces reinforcement.

6 Conclusions

In this project a mean to increase the maximum acceleration of a shake table was successfully created. The addon provided successfully 2.9 times time history acceleration amplification when no additional weight was set and 1.7 times amplification when the wood frame was set on its top. The development process highlight a special need of heed for the quality of connecting parts and the tuned mass damper behavior study, further improve of this addon structure is needed though. Reduction of the rocking motion as well as strong tuned mass damper behavior obtained when the wood frame was set are both needed to obtain a totally reliable amplifying structure. However, created numerical model provide good mean to anticipate this specific behavior for the preparation of further experiment using this passive structure. Considering the created addon with its actual capacity, acceleration as high as the one recorded at MYG004 Tsukidate during 2011 Tohoku earthquake could be successfully input on light weight specimen. These light weight specimen could be for exemple shelves in the case of furniture toppling study or structural parts such as the on for reinforced concrete wall study.

The Japanse wood frame structural experiment showed that despite the strong acceleration that was input on the structure, the frequency content of the input had primordial impact to the structural damage creation. Therefore relative velocity and displacement must have stronger influence on the wood frame behavior than acceleration. This result does not consist in an empirical proof that MYG004 ground motions cannot create any damage on Japanese traditional wood frame as the reproduced acceleration was still lower input than the actual recorded one. However, the low acceleration that was observed on the top of the wood frame when the maximum acceleration reached 1400 gal accentuate the possibility of such high acceleration occurrence without any creation of damage. This results is pleading on the need to decrease the influence of high frequency in the calculation of JMA intensity, and JMA intensity on input on the wood frame signal should be calculated.

In addition the wood frame using wall of columns system with side braces showed some good capacity to resist the high acceleration and high velocity of JMA Kobe signal. Even after 120% intensity of that input signal the structure remained safe. This kind of reinforcement is balancing both disadvantage of the extreme behavior of independently considered reinforcement techniques, the loss of stiffness for the braces and the increase of stiffness for the wall of columns .

Bibliography

[1] GOTO H., MORIKAWA H. 2012. Ground motion characteristics during the 2011 off the Pacific Coast of Tohoku Earthquake *Soils and Foundations, 52 : 769-779*

[2] AIJ RECONNAISSANCE COMMITTEE. 2012. Preliminary Reconnaissance Report of the 2011 Tohoku Chiho Taiheiyo-Oki Earthquake chap 2.1 *Architectural Institute of Japan Editor, Springer 978-4-431-54097-7*

[3] MOTOSAKA M. 2012. Lessons of the 2011 Great East Japan Earthquake focused on characteristics of ground motions and building damage *Proceeding of the International Symposium on Engineering lessons learned from the 2011 Great East Japan Earthquake, March 2012.*

[4] MOTOSAKA M., MITSUJI K. 2012. Building damage during the 2011 off the Pacific coast of Tohoku earthquake *Proceeding of the International Symposium on Engineering lessons learned from the 2011 Great East Japan Earthquake, March 2012.*

[5] HAYAKAWA T., SATOH T., OSHIMA M. 2012. Estimation of the nonlinearity of the surface soil at Tsukidate during the 2011 off the Pacific coast of Tohoku Earthquake *15 WCEE Lisboa 2012.*

[6] NAGASHIMA F., MATSUSHIMA S., KAWASE H. ET AL. 2014. Application of Horizontal-to-Vertical spectral ratios for earthquake ground motions to identify subsurface structures at and around K-NET site in Tohoku, Japan. *Bulletin of the Seismological Society of America, Vol. 104 No. 5, pp. 2288-2302*

[7] NAGASHIMA F., MATSUSHIMA S., KAWASE H. ET AL. 2014. Application of H/V spectral ratios for earthquake ground motions and microtremors at K-NET sites in Tohoku region, Japan to delineate soil nonlinearity during the 2011 off the Pacific coast of Tohoku Eartquake *Proceeding of the International Symposium on Engineering lessons learned from the 2011 Great East Japan Earthquake, March 2012.*

[8] JEONG S. 2013. Topographic amplification of seismic motion including nonlinear response *Academic thesis, Georgia Institute of Technology.*

[9] YOSHIDA Y., UENO H., ET AL. 2011. Source process of the 2011 of the Pacific coast of Tohoku Earthquake with the combination of teleseismic and strong motion data *Earth Planet Space, 63 : 565-569*

[10] HARTZELL S. H. 1978. Eartquake aftershocks as Green's fuctions *Geophys. Res. lett., 5,1-4*

[11] IRIKURA K. 1986 Prediction of strong acceleration motions using empirical Green's funstion method *Proc. 7th Jpn Earthq. Eng. Symp., 151-156*

[12] MIYAKE H.T., IWATA T., IRIKURA K. 2003. Source characterization for broadband ground-motion simulation : Kinematic heterogeneous source model and strong motion generation area *Bull. Seismol. Soc. Am., 93, 2531-2545*

[13] ASANO K., IWATA T. 2012. Source model for strong ground motion generation in the frequency range 0.1-10Hz during the 2011 Tohoku earthquake *Earth Planets Space, 64,1111-1123*

[14] YAMAGUCHI N., YAMAZAKI F. 2001. Estimation of strong motion distribution in the Kobe earthquake based on building damage data. *Earthquake Engineering Struct. Dyn., 30 : 787-801*

[15] NCEER TEAM. 1995. Preliminary Reports from the Hyogo-ken Nambu Earthquake of January 17, 1995 *NCEER reconnaissance report*

[16] ANSHEL J.S. 1998. Hyogoken-Nanbu (Kobe) Earthquake of January 17, 1995. Lifeline Performance *ASCE : Technical council on Lifeline Earthquake Engineering, Monograph No. 14*

[17] NILIM-PWRI TEAM. 2004. Report on Damage to Infrastructure by the Mid Niigata Prefecture Earthquake in 2004 *NILIM-PWRI Joint Reconnaissance Team*

[18] KONAGAI K. 2004. Preliminary Report : Mid-Niigata Prefecture Earthquake. Preliminary report on damage caused by the Mid-Niigata prefecture earthquake on Octobe 23, 2004 *Japan Society of Civil Engineers JSCE report*

[19] KARIM K.R., YAMAZAKI F. 2002. Correlation of JMA instrumental seismic intensity with strong motion parameters *Earthquake engineering and structural dynamics, 31 : 1191-1212*

[20] KAWASE H., 2006. Site effects derived from spectral inversion method fo K-NET,KiK-net, and JMA Strong Motion Network with special reference to soil nonlinearity in high PGA records *Bull. Earthq. Res. Inst., Vol. 81 pp.309-315*

[21] MOTOSAKA M.,NAGANO M., 1993. Dynamic partial uplift analysis of a structure on a 3-D layered half space based on recursive evaluation of interaction forces using dynamic stiffness of the unbounded soil in frequency domain. *Journal of Structural and Construction Engineering AIJ 45, 79-88*

APPENDIX 1 : Detailed plans of the shake table add-on first design

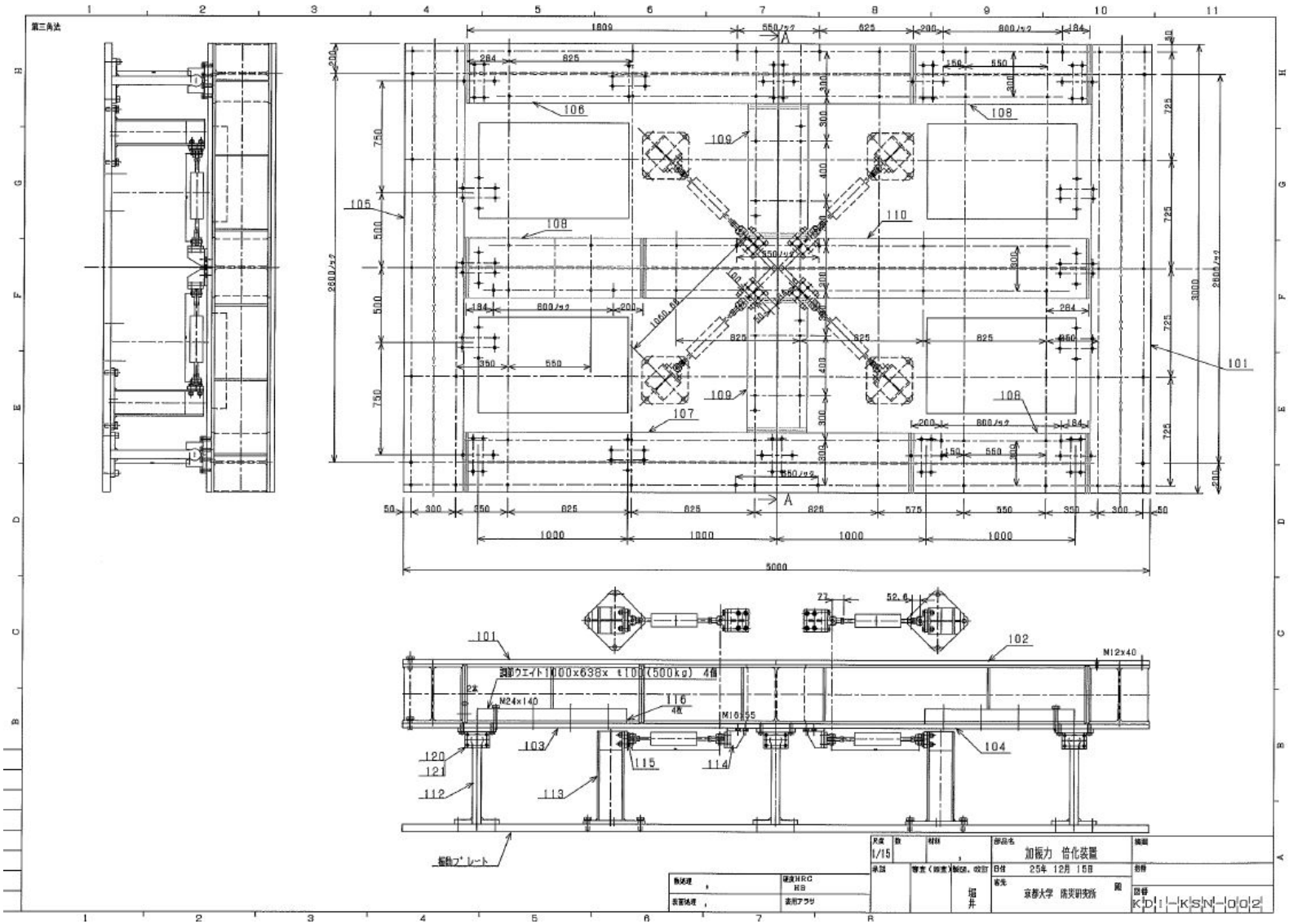

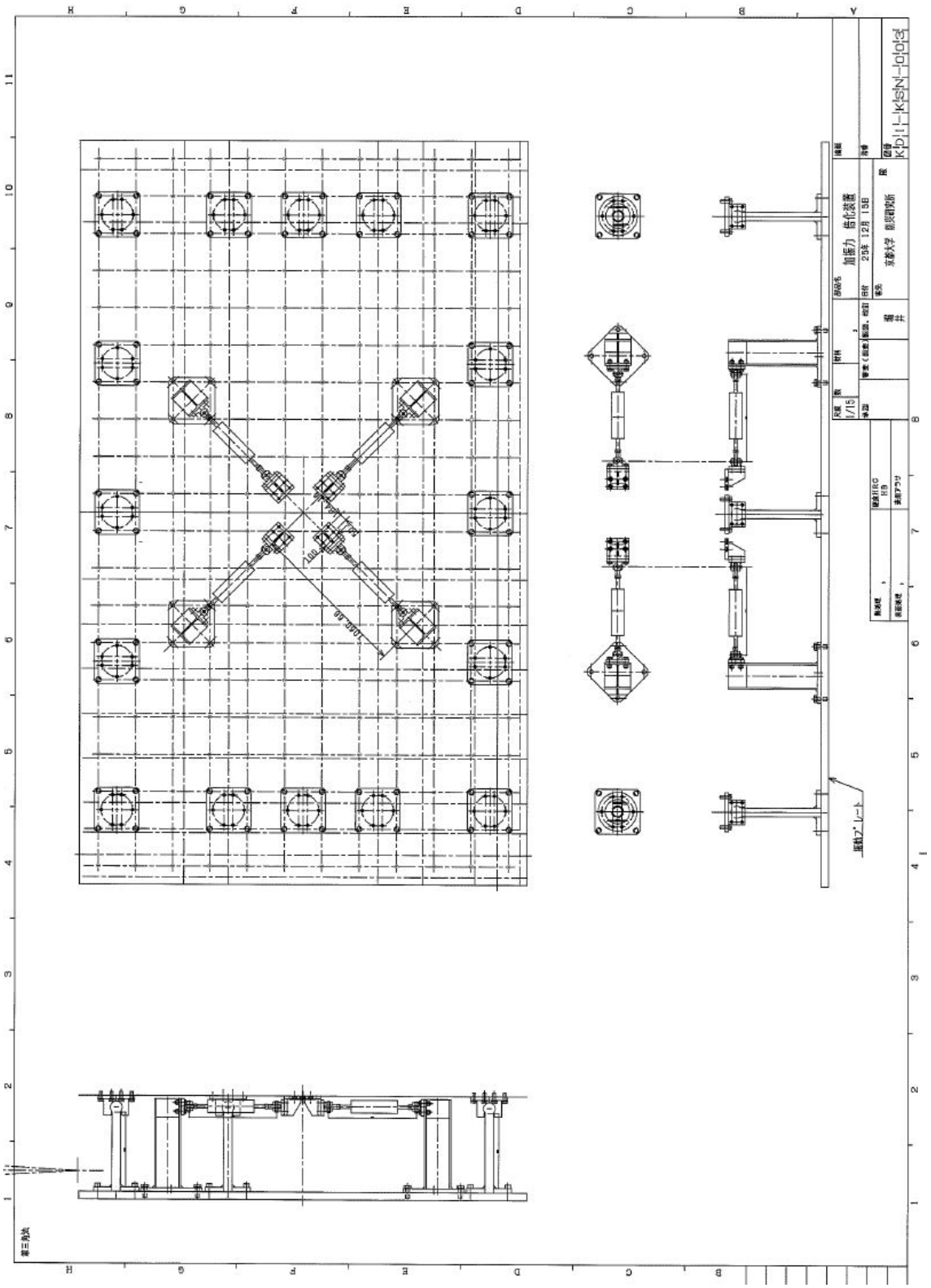

Predoctoral year of research

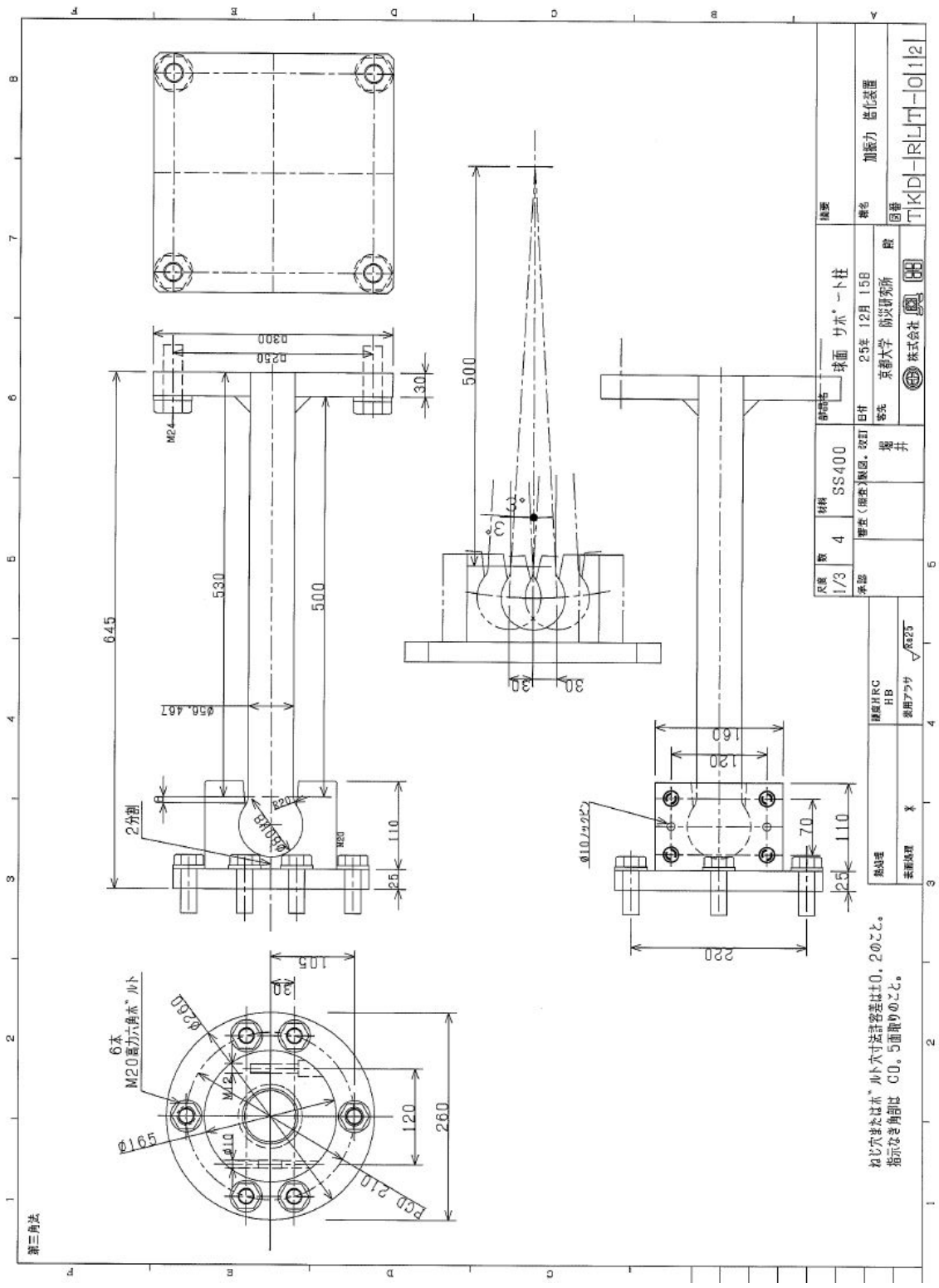

Predoctoral year of research

APPENDIX 2 :

Damage observation after JMA Kobe 120% is input on the wood frame with a wall of columns reinforcement and side braces

Figure 57: Pulled down bottom beam of the wall of columns

Figure 58: Cracked braces at its connection with the frame column